Project 2312/A5

Numerical Modelling Of Fringing Fields And Their Use For Complex Permittivity Measurements At High Frequencies

March 1992

Progress Report for Period February 1991 to February 1992

By

Camelia Gabriel
Department of Physics
King's College, University of London

REPORT DOCUMENTATION PAGE

Form Approved
OMB No. 0704-0188

1. AGENCY USE ONLY (Leave blank)	2. REPORT DATE	3. REPORT TYPE AND DATES COVERED
	March 1992	First Technical Report Feb 91-Jan 92 Annual

4. TITLE AND SUBTITLE
Numerical modelling of fringing fields and their use for complex permittivity measurements at high frequencies

5. FUNDING NUMBERS
F
PE- 61102F
PR - 2312
TA - A5

6. AUTHOR(S)
Camelia Gabriel

7. PERFORMING ORGANIZATION NAME(S) AND ADDRESS(ES)
Kings College
Department of Physics
Strand
London WC2R 2LS

8. PERFORMING ORGANIZATION REPORT NUMBER

9. SPONSORING/MONITORING AGENCY NAME(S) AND ADDRESS(ES) Dr Cornette
Sponsoring Agency: Air Force Office of Scientific Research
Bolling AFB, DC/NL
Sponsoring/Monitoring Agency: European Office of Aerospace Research and Development
PSC 802, Box 14, FPO, AE 09499-0200

10. SPONSORING/MONITORING AGENCY REPORT NUMBER
AFOSR-91-0122

11. SUPPLEMENTARY NOTES

12a. DISTRIBUTION/AVAILABILITY STATEMENT
Approved for Public Release
Distribution Unlimited

12b. DISTRIBUTION CODE

13. ABSTRACT (Maximum 200 words)

Interest in the use of open ended coaxial probes for dielectric measurements stems from their suitability to a variety of applications in material science, chemical, biochemical and biomedical fields. This report deals with the theoretical principles involved in the implementation of this technique and the simplifying assumptions adopted in practice. A rigorous formulation based on transmission line theory will be derived and compared to a number of simpler models reported in the literature and used for dielectric measurements with various degrees of success.

14. SUBJECT TERMS
Complex permittivity, non-destructive measurement

15. NUMBER OF PAGES
19

16. PRICE CODE

17. SECURITY CLASSIFICATION OF REPORT	18. SECURITY CLASSIFICATION OF THIS PAGE	19. SECURITY CLASSIFICATION OF ABSTRACT	20. LIMITATION OF ABSTRACT
Unclassified	Unclassified	Unclassified	Unclassified

GENERAL INSTRUCTIONS FOR COMPLETING SF 298

The Report Documentation Page (RDP) is used in announcing and cataloging reports. It is important that this information be consistent with the rest of the report, particularly the cover and title page. Instructions for filling in each block of the form follow. It is important to *stay within the lines* to meet *optical scanning requirements*.

Block 1. Agency Use Only *(Leave blank)*.

Block 2. Report Date. Full publication date including day, month, and year, if available (e.g. 1 Jan 88). Must cite at least the year.

Block 3. Type of Report and Dates Covered. State whether report is interim, final, etc. If applicable, enter inclusive report dates (e.g. 10 Jun 87 - 30 Jun 88).

Block 4. Title and Subtitle. A title is taken from the part of the report that provides the most meaningful and complete information. When a report is prepared in more than one volume, repeat the primary title, add volume number, and include subtitle for the specific volume. On classified documents enter the title classification in parentheses.

Block 5. Funding Numbers. To include contract and grant numbers; may include program element number(s), project number(s), task number(s), and work unit number(s). Use the following labels:

C	- Contract	PR	- Project
G	- Grant	TA	- Task
PE	- Program Element	WU	- Work Unit Accession No.

Block 6. Author(s). Name(s) of person(s) responsible for writing the report, performing the research, or credited with the content of the report. If editor or compiler, this should follow the name(s).

Block 7. Performing Organization Name(s) and Address(es). Self-explanatory.

Block 8. Performing Organization Report Number. Enter the unique alphanumeric report number(s) assigned by the organization performing the report.

Block 9. Sponsoring/Monitoring Agency Name(s) and Address(es). Self-explanatory.

Block 10. Sponsoring/Monitoring Agency Report Number. *(If known)*

Block 11. Supplementary Notes. Enter information not included elsewhere such as: Prepared in cooperation with...; Trans. of...; To be published in.... When a report is revised, include a statement whether the new report supersedes or supplements the older report.

Block 12a. Distribution/Availability Statement. Denotes public availability or limitations. Cite any availability to the public. Enter additional limitations or special markings in all capitals (e.g. NOFORN, REL, ITAR).

- DOD - See DoDD 5230.24, "Distribution Statements on Technical Documents."
- DOE - See authorities.
- NASA - See Handbook NHB 2200.2.
- NTIS - Leave blank.

Block 12b. Distribution Code.

- DOD - Leave blank.
- DOE - Enter DOE distribution categories from the Standard Distribution for Unclassified Scientific and Technical Reports.
- NASA - Leave blank.
- NTIS - Leave blank.

Block 13. Abstract. Include a brief *(Maximum 200 words)* factual summary of the most significant information contained in the report.

Block 14. Subject Terms. Keywords or phrases identifying major subjects in the report.

Block 15. Number of Pages. Enter the total number of pages.

Block 16. Price Code. Enter appropriate price code *(NTIS only)*.

Blocks 17. - 19. Security Classifications. Self-explanatory. Enter U.S. Security Classification in accordance with U.S. Security Regulations (i.e., UNCLASSIFIED). If form contains classified information, stamp classification on the top and bottom of the page.

Block 20. Limitation of Abstract. This block must be completed to assign a limitation to the abstract. Enter either UL (unlimited) or SAR (same as report). An entry in this block is necessary if the abstract is to be limited. If blank, the abstract is assumed to be unlimited.

TABLE OF CONTENTS

1.INTRODUCTION..... 2

2.THEORETICAL ANALYSIS..... 3
2.1 Description of the problem..... 3
2.2 Expression for the electric and magnetic fields inside the line..... 3
2.3 Expression for the electric and magnetic fields outside the line..... 5
2.4 Expression for the terminating admittance..... 5

3. NUMERICAL TECHNIQUES..... 6
3.1 Full solution using MOM..... 6
3.2 Simplified variational methods..... 6
3.2.Alternative variational method 8

4. PREDICTION OF MODELS..... 10

5. DIELECTRIC MEASUREMENTS..... 11

6. SUMMARY AND FUTURE WORK..... 11

7. REFERENCES..... 12

. FIGURES
Figure 1.Cylindrical coordinates of a coaxial probe probe
Figure 2. Illustration of the extrapolation technique
Figure 3. Derivation of admittance models
Figure 4. (a) Real and (b) imaginary parts of the admittance of a coaxial probe in methanol at 20°C
Figure 5. (a) Real and (b) imaginary parts of the admittance of a coaxial probe in water at 20°C
Figure 6. (a) Real and (b) imaginary parts of the admittance of a coaxial probe in formamide at 20°C
Figure 7. (a) Real and (b) imaginary parts of the admittance of a coaxial probe in water at 23.8°C. The joined symbols are experimental measurements and the solid lines the predictions of the two models
Figure 8 Measured and calculated values of the complex admittance of the probe in contact with water at 20 °C and in the frequency range 100 MHz to 20 GHz
Figure 9: Measured (symbols) and literature values of the complex permittivity of formamide at 20°C

1. INTRODUCTION

This progress report describes the work performed in the first year of Project 2312/A5 under Grant AFOSR-91-0122. The aim of this project is to provide a theoretical basis for the use of open ended coaxial probes for dielectric measurements. More specifically we had three main objectives:

1. To model the fringing fields of coaxial sensors in lossy media in order to determine the extent of the fringing field penetration into homogeneous or laminar samples.

2. To develop an admittance model for the probe in lossy media and a numerical technique that enable its use for dielectric measurements.

3. To evaluate the sources of error associated with the technique and to develop an error model to estimate the sensitivity of the measurements at each frequency.

Interest in the use of open ended coaxial probes for dielectric measurements stems from its suitability to a variety of applications in material science, chemical, biochemical and biomedical fields. Its acceptability as a rigorous measurement technique awaits a full understanding of the theoretical principles involved. We are currently working on such a study and will be presenting our preliminary findings in this report. The theoretical study required for the development of an admittance model has now been completed and will serve as a basis for the study of field penetration in lossy dielectric. The assessment of the errors associated with will be carried out in the very near future.

Our studies show that the simpler admittance models more commonly used for dielectric measurements can be derived from our rigorous formulation provided certain simplifying assumptions are made. The full solution presented in this report provides a unifying theory for a number of models reported in the literature and used for dielectric measurements with various degrees of success[1-3]. We have studied three relatively simpler model and will be reporting on their range of applicability and their limitations.

THEORETICAL ANALYSIS

2.1 Description Of The Problem

For the purpose of this analysis the coaxial probe is assumed to be axisymmetric, fitted with a ground plane that is large by comparison to its diameter and that in addition to the principal TEM mode only TM_{0n} evanescent modes that preserve cylindrical symmetry are generated at the interface.

The problem is therefore best described in the cylindrical coordinate system (ρ, ϕ, z) as illustrated in Figure 1 in which the ε_1 refers to the permittivity of the dielectric medium inside the line and ε_2 outside the line , ρ is the radial distance from the axis, ϕ the angular displacement around the axis and z the displacement along the axis. In the first instance we will assume that the medium outside the probe is uniform and occupies the entire half-space beyond the ground plate. It may be appropriate to mention at this stage, that our future plans include making a modification to the formulation to treat the case of a dielectric material of finite thickness, backed by an infinite perfectly conducting sheet parallel to the ground plane.

2.2 Expression For The Electric And Magnetic Fields Inside The Line

The field inside the line are a superposition of the forward travelling fundamental TEM mode, its reflection at the interface and the TM_{0n} evanescent modes generated at the discontinuity. Their derivation, in terms of a potential Φ, from Maxwell's equations yields

$$H_\varphi(\rho,z) = \frac{1}{\eta_1\rho}a_0\left[e^{-jk_1z} - \Gamma e^{jk_1z}\right] + \sum_{n=1}^{\infty}\left(\frac{-j\omega\varepsilon_1}{\gamma_n}\right)a_n e^{\gamma_n z}\frac{d\Phi_n(\rho)}{d\rho}, \qquad (1)$$

$$E_\rho(\rho,z) = \frac{1}{\rho}a_0\left[e^{-jk_1z} - \Gamma e^{jk_1z}\right] + \sum_{n=1}^{\infty}a_n e^{\gamma_n z}\frac{d\Phi_n(\rho)}{d\rho}, \qquad (2)$$

$$E_z(\rho,z) = \sum_{n=1}^{\infty} \left(\frac{-p_n}{\gamma_n}\right) a_n e^{\gamma_n z} \Phi_n(\rho) \quad , \qquad (3)$$

in which

Γ is the reflection coefficient of the TEM mode, γ_n is the propagation constant of mode n

$$\gamma_n = [\, p_n^2 \; - k_1^2]^{1/2}$$

$$k_1^2 = \omega^2 \mu_1 \varepsilon_1$$

ω is the angular frequency and η_1 ,the intrinsic impedance is

$$\eta_1 = \sqrt{\mu_1 / \varepsilon_1}$$

for $n > 0$ p_n are the n roots of

$$J_0(p_n b)\, Y_0(p_n a) - J_0(p_n a)\, Y_0(p_n b) = 0$$

where J_0, Y_0 are the Bessel's functions of the first and second kinds of order zero, a and b the radii of the coaxial line.

for n=0 (TEM mode) $p_0 = 0$

For each n, the function Φ_n is defined for each mode as

$$\Phi_n(\rho) = J_0(p_n \rho)\, Y_0\,(p_n a) - J_0\,(p_n a)\, Y_0\,(p_n \rho)$$

with

$$\Phi_n(a) = \Phi_n(b) = 0$$

a_0 and a_n are amplitude terms normalised to the dimensions of the line and can be expressed in terms of the magnitude of the electric field at the aperture $E_\rho^{\,a}(\rho)$ at z=0 as

$$a_0 = \int_a^b E_\rho^a(\rho) d\rho \,/\, (1+\Gamma)\ln(b/a)$$

and

$$a_n = \int_a^b \frac{d\Phi_n(\rho)}{d\rho} \rho\, E_\rho^a\,(\rho) d\rho \,/ \int_a^b \left[\frac{d\Phi_n(\rho)}{d\rho}\right]^2 \rho\, d\rho$$

with

2.3 Expression For The Electric And Magnetic Fields outside The Line

In dielectric medium 2 ($z > 0$) the magnetic field is expressed in terms of the electric field $E_\rho^a(\rho)$ at the aperture as

$$H_\varphi^+(\rho) = \frac{j\omega\varepsilon_2}{2\pi}\int_a^b\int_0^{2\pi} E_\rho^a(\rho')\cos(\varphi'-\varphi)\frac{e^{-jk_2R}}{R}\rho' d\varphi' d\rho' \tag{4}$$

where ρ' and φ' refer to the coordinates of a source point at the aperture and R the distance from the source to the corresponding field point which at z=0 gives

$$R^2 = \rho^2 + \rho'^2 - 2\rho\rho'\cos(\varphi'-\varphi).$$

The aperture field $E_\rho^a(\rho)$ at z=0 can be expressed from (2) as

$$E_\rho^a(\rho) = \frac{1}{\rho}a_0(1+\Gamma) + \sum_{n=1}^{\infty} a_n \frac{d\Phi_n(\rho)}{d\rho} \tag{5}$$

2.4 Expression For The Terminating Admittance

Assuming a continuity of $E_\rho^a(\rho)$ at the interface the continuity of H_φ which across the plane z=0 allows H_φ^+ (1) to be equated to H_φ^- (4) which gives

$$\frac{1}{\eta_1\rho}a_0(1-\Gamma) + \sum_{n=1}^{\infty}\left(\frac{-j\omega\varepsilon_1}{\gamma_n}\right)a_n\frac{d\Phi_n(\rho)}{d\rho} = \frac{j\omega\varepsilon_2}{2\pi}\int_a^b\int_0^{2\pi} E_\rho^a(\rho')\cos(\varphi'-\varphi)\frac{e^{-k_2R}}{R}\rho' d\varphi' d\rho' \tag{6}$$

Substituting for a_o and introducing the terminating admittance Y^a of a coaxial line which is defined as

$$Y^a = Y_0\left(\frac{1-\Gamma}{1+\Gamma}\right),$$

where Y_0 is the characteristic admittance of the coaxial line

$$Y_0 = \frac{2\pi}{\eta_1 \ln(\frac{b}{a})}.$$

Equation (6) can be re-written as

$$\frac{1}{2\pi\rho}\int_a^b E_\rho^a(\rho)d\rho Y^a = \sum_{n=1}^{\infty} \frac{j\omega\varepsilon_1}{\gamma_n}\frac{d\Phi_n(\rho)}{d\rho}a + \frac{j\omega\varepsilon_2}{2\pi}\int_a^b\int_0^{2\pi} E_\rho^a(\rho')\cos(\varphi'-\varphi)\frac{e^{-jk_2R}}{R}\rho' d\varphi' d\rho'$$

$$Y^a = \frac{1}{A}\sum_{n=1}^{\infty} \frac{j\omega\varepsilon_1}{\gamma_n}\frac{d\Phi_n(\rho)}{d\rho} + \frac{j\omega\varepsilon_2}{2\pi}\int_a^b\int_0^{2\pi} E_\rho^a(\rho')\cos(\varphi'-\varphi)\frac{e^{-jk_2R}}{R}\rho' d\varphi' d\rho' \quad (7)$$

where

$$A = \frac{1}{2\pi\rho}\int_a^b E_\rho^a(\rho)d\rho$$

The admittance Y^a and therefore also the reflection coefficient Γ can be calculated from equation 7 using a appropriate numerical technique. We have used a method of moment technique (MOM) for a full solution of equation(7).

3. NUMERICAL TECHNIQUES

3.1 Full Solution Using MOM

The MOM solution is based on the assumption that since the aperture field is φ independent then within a small concentric ring of radius ρ_k and ρ_{k+dk} the potential $V_k(\rho)$ is constant. The region between the radii of the coaxial probe a and b is subdivided into N intervals with boundaries at ρ_0=a at which V_k=1, ρ_N=b.at which V_k=0.

The above assumption is valid if dk is infinitesimally small which require N=∞. A finite number of rings N will inevitably introduce a truncation error. To overcome the problem we have introduced a quadratic extrapolation technique[4] to calculate the admittance or reflection coefficient corresponding to N=∞ from calculation at three finite values of N. Figure 2 shows the intermediate and extrapolated results of reflection coefficient for a hypothetical measurement configuration of a coaxial line with a=2.333mm, b=7.549mm $\varepsilon_1/\varepsilon_o$=2.15 and $\varepsilon_2/\varepsilon_o$=100-j100 at 1GHz. This rather odd combination of parameters was chosen to allow for comparison with equivalent values in reference 4. The agreement was found to be of the order of

10^{-6} and was deemed satisfactory.

3.2 Simplified Variational Methods

The equation (7) can be simplified by assuming that $E_\rho^a(\rho)$ is inversely proportional to ρ, i.e.

$$E_\rho^a(\rho) = \frac{E_0}{\rho} \tag{8}$$

where E_0 is a constant. Incorporating assumption (8) and some lengthy but straightforward algebraic manipulations (7) becomes

$$\frac{E_0^2}{2\pi}\left[\int_a^b \frac{d\rho}{\rho}\right]^2 Y^a = j\omega\varepsilon_1 \sum_{n=1}^{\infty} \frac{E_0^2}{\gamma_n}\left[\Phi_n(b) - \Phi_n(a)\right]^2 \frac{1}{\int_a^b \left[\frac{d\Phi_n(\rho)}{d\rho}\right]^2 \rho d\rho}$$

$$+ \frac{j\omega\varepsilon_2 E_0^2}{2\pi}\int_a^b\int_a^b\int_0^{2\pi} \cos(\varphi' - \varphi)\frac{e^{-k_2 R}}{R} d\varphi' d\rho' d\rho \tag{9}$$

The terms of the n summation in (9) are equal to zero which gives an aperture admittance Y^a expressed as

$$Y^a = \frac{j\omega\varepsilon_2}{[\ln(b/a)]^2}\int_a^b\int_a^b\int_0^{2\pi} \cos(\varphi' - \varphi)\frac{e^{-k_2 R}}{R} d\varphi' d\rho' d\rho \tag{10}$$

This expression can be determined by expanding the exponential term into an infinite series in the form

$$Y^a = \omega C_o\{\varepsilon^* C_1 + \varepsilon^{*2} C_3\omega^2 + \varepsilon^{*5/2} C_4\omega^3 + \varepsilon^{*3} C_5\omega^4 + \varepsilon^{*7/2} C_6\omega^5 + \varepsilon^{*4} C_7\omega^6$$
$$+ \varepsilon^{*9/2} C_8\omega^7 + \varepsilon^{*5} C_9\omega^8 + \varepsilon^{*11/2} C_{10}\omega^9 + \ldots\} \tag{11}$$

were the C terms are constants determined by the dimensions of the line only

We have used expression (11) for dielectric measurements[5] and found that, in practice, including more than 10 terms had no effect on the solution. For a 50 Ω Teflon-filled coaxial probe (3.5 mm OD, a = 0.456 mm, b = 1.490 mm, $\varepsilon_c/\varepsilon_o$ = 2.1) commonly used for high

frequency measurements, equation (11) fails to converge for frequencies in excess of 7 GHz for lossy dielectric.

It is interesting to note that by truncating the series after one term only and dropping the higher order terms of ω. Equation (11) becomes[5]

$$Y^a = \frac{8j\omega\varepsilon_2}{[\ln(b/a)]^2}(a+b)[E(m)-1] \tag{12}$$

where E(m) is the complete elliptic integral of the second kind which can be approximated by a polynomial, and

$$m = \frac{4ab}{(a+b)^2}.$$

The expression (12) can thus be written as

$$Y^a = j\omega C\varepsilon_2$$

and is equivalent to describing the admittance of the probe in terms of a frequency independent lumped capacitance term. Because of it simplicity formulations equivalent to equation (12) have been widely used for dielectric measurements.

3.2 Alternative Variational Method

The simplifying assumption that $E_\rho{}^a(\rho)$ is inversely proportional to ρ, is implicit in (10) and in the previous section we have shown that it can be solved by expanding the exponential term. An alternative solution would be to express the φ' integral in terms of Bessel functions which gives[6] after changing the integration parameters

$$Y^a = Y_0 \frac{jk_2}{\ln(b/a)} \int_0^\infty \frac{-\xi}{(\xi^2 - k_2^2)^{1/2}} \left[\int_a^b J_1(\xi\rho)d\rho\right]^2 d\xi$$

$$\arg(\xi^2 - k_2^2)^{1/2} = \begin{cases} 0, & \xi > k_2 \\ -\dfrac{\pi}{2}, & \xi < k_2 \end{cases}.$$

Evaluating the ρ integral gives

$$Y^a = Y_0 \frac{jk_2}{\ln(b/a)} \int_0^{\infty} \frac{1}{\xi(\xi^2 - k_2^2)^{1/2}} [J_0(\xi b) - J_0(\xi a)]^2 d\xi \qquad (13).$$

The integral is considered separately over the ranges $0<\xi<k_2$ and $k_2<\xi<\infty$. The integrand changes from imaginary to real at $\xi=k_2$, and the integration over these two ranges gives the aperture conductance G and susceptance B respectively. For $0<\xi<k_2$, the variable of integration is changed to $\xi=k_2 \sin\theta$ while for $k_2<\xi<\infty$, the present infinite integral can be expressed as a finite integral of integral sines. Given that for the coaxial probe

$$Y^a = G + jB$$

The solution of (13) gives

$$G = \frac{Y_0 \sqrt{\varepsilon^*}}{\ln(b/a)\sqrt{\varepsilon_c}} \int_0^{\pi/2} \frac{1}{\sin\theta} \left[J_0\left(k_0 \sqrt{\varepsilon^* b \sin\theta}\right) - J_0\left(k_0 \sqrt{\varepsilon^* a \sin\theta}\right)\right]^2 d\theta \qquad (14a)$$

$$B = \frac{Y_0 \sqrt{\varepsilon^*}}{\pi \ln(b/a)\sqrt{\varepsilon_c}} \int_0^{\pi} \left[2Si\left(k_0\sqrt{\varepsilon^*(a^2 + b^2 - 2ab\cos\theta)}\right) - 2Si\left(2k_0\sqrt{\varepsilon^* a \sin\left(\frac{\theta}{2}\right)}\right) - 2Si\left(2k_0\sqrt{\varepsilon^* b \sin\left(\frac{\theta}{2}\right)}\right)\right] d\theta \qquad (14b)$$

where k_o is the propagation constant in free space, ω/c, ε^* refers to medium 2 ; J_o is the Bessel function of order zero; and Si is the sine integral.

The admittance model described in (14a) and (14b) is, in principle, identical to that described by (11) since both originate from (10). The only difference is the numerical technique used for the solution.

A summary of the derivation of the models is given in figure 3.

4. PREDICTIONS OF ADMITTANCE MODELS

The predictions of models developed in the previous section will be compared with each other and then validated against measured admittance values and finally used to perform dielectric measurements on standard solutions. The experimental work was performed on an HP 8720 network analyser in the frequency range 130 MHz to 20 GHz using a 50 Ω Teflon-filled coaxial probe (3.5 mm OD, a = 0.456 mm, b = 1.490 mm, $\varepsilon_c/\varepsilon_o$ = 2.1, 21 mm ground plane).

The models described by equations 10, 12 and 14 were studied in details in a previous report[5]. Its main findings were as follows:

1. For the probe in a lossless medium, the three models were in agreement with each other and with the measured admittance for frequencies up to 20 GHz.

2. In a lossy medium, the predictions of the models were in agreement up to about 3 GHz, equations 10 and 14 were in agreement for frequencies up to 7 GHz.

3. Equations 14 gave the best agreement with experimental results over the frequency range studied.

The aim of this report is to describe the performance of the newly developed model (equation 7) and to compare it to the simpler formulations. Two of the previous models (10 and 12) were found unsuitable for high frequency work and will no longer be mentioned. The performance of the new model will be compared to equations 14 only.

Figures 4 to 6 show a comparison between the predictions of equations (7) and (14) for the real and imaginary part of the admittance of the probe in standard liquids at 20°C in the frequency range 100 MHz to 20 GHz. The measurements were obtained with the network analyser calibrated using the manufacturer's standards prior to connecting the probe.

The predictions of both models exhibit the main features of the standard liquids measured. There are, however, systematic differences betweem the two models and between them and the experimental values. It important to mention that the experimental values depends on the properties of the standard liquids as well as the probe and connector. To illustrate this point measurements on water, with two different probes, are reported in Figure 7 showing clearly that the experimental values fall in between the predictions of the models.

5. DIELECTRIC MEASUREMENTS

The analysis of the admittance models in section 4 suggests the techniques are not suited to absolute measurements with a network analyser calibrated using factory standards. The models assume a perfect coaxial probe and do not account for the unwanted reflections of the connector. The limitation of the models and the effect of the probe and connector can be eliminated if either model is used as part of a calibration at the end of the probe. This is illustrated in Figure 8 were the predictions of equations 14 a &b are compared to the measured values.

Using the end of probe calibration technique both models were successfully used for the measurement of the dielectric properties of standard liquids. Figure 9 shows the agreement between the measurements using the two models and the literature values for formamide at 20°C.

Experimentally, the main difference between the models is in the computation time. Using an HP345 work station, it takes less than a minute to compute the dielectric properties at 21 frequency points using equations 14. It takes approximately 3 minutes per frequency point using the model described by equation 7.

6 SUMMARY AND FUTURE WORK

The aims of this project are:

1. Development of admittance models incorporating the excitation of TEM and higher order modes at the probe-sample interface.
2. Coaxial probe field penetration in lossy media;
3. Error analysis and model evaluation

Most of the work related to 1 and 2 above have now been completed. We plan to carry out the error analysis in the near future before embarking on a series of dielectric measurements using the new techniques. The material under consideration are liquid crystals and conductive plastics.

Finally, we plan to write two or more publications based on the material produced during the project.

6. REFERENCES

1. Misra, D.K. A quasi-static analysis of open-ended coaxial lines. IEEE Trans Microwave Theory Tech **MTT-35**: 925-928 (1987).

2. Misra, D., M. Chabbra, B.R. Epstein, M. Mirotznik, and K.R. Foster. Noninvasive electrical characterisation of materials at microwave frequencies using an open-ended coaxial line: Test of an improved calibration technique. IEEE Trans Microwave Theory Tech **MTT-38**: 8-14 (1990).

3. Gabriel, C., E.H. Grant, and I.R. Young. Use of time domain spectroscopy for dielectric measurements with a coaxial probe, J Phys E: Sci Instrum, **19**: 843-846 (1986).

4. Jenkins, S ,Preece, A.W., Hodgetts, T.E, Symm, G.T.,. Warham,A.G.P,. Clarke,R.N Comparison of three numerical treatments for the open-ended coaxial line sensor, Electronics Letters, **26**: .234-236 (1990).

5. Gabriel, C Permittivity probe modelling, USAF report (1991)

6.Galejs, J., Antennas in Homogeneous Media, Oxford, England: Pergamon (1969).

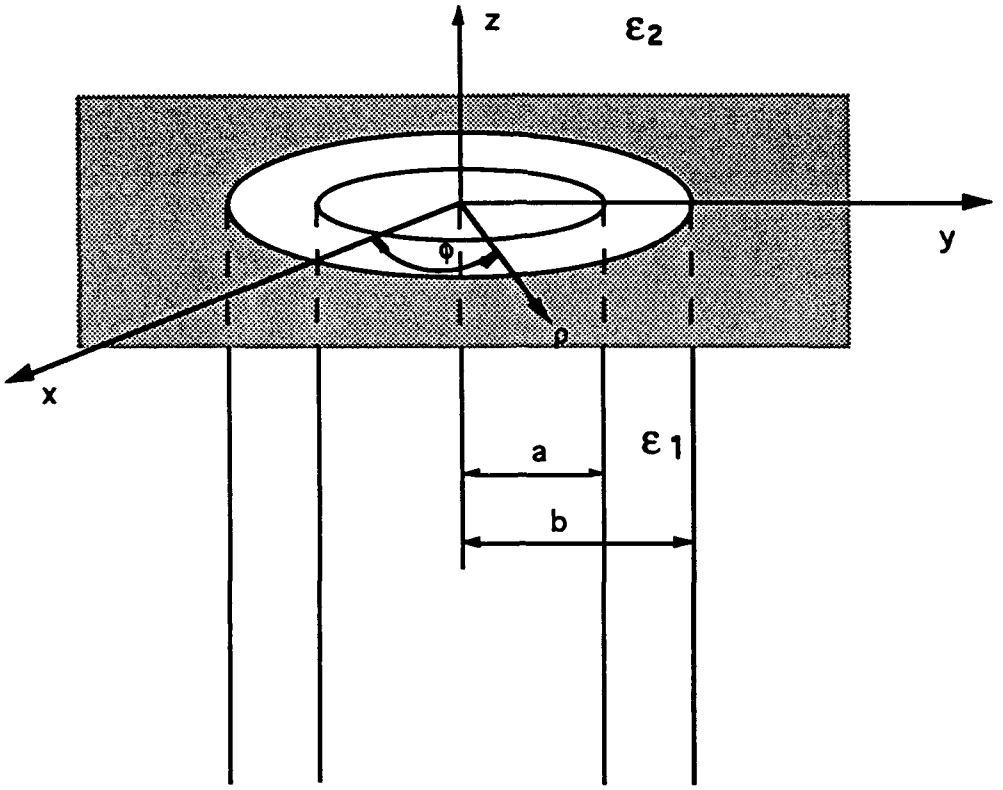

Figure 1.Cylindrical coordinates of a coaxial probe probe on inner and outer radii a and b respectively.

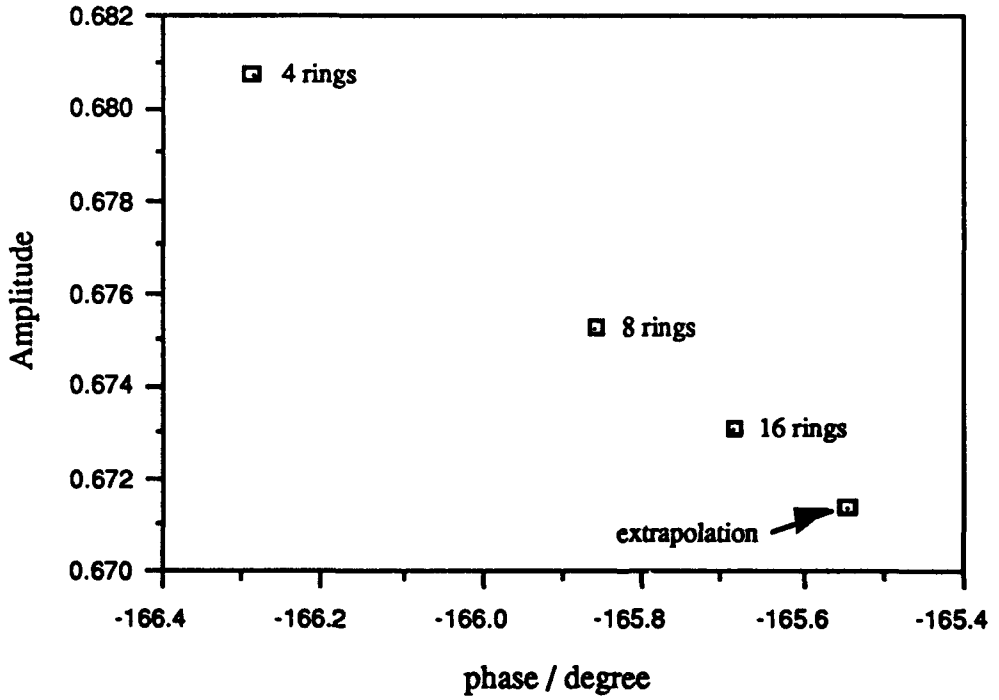

Figure 2 Illustration of the extrapolation technique

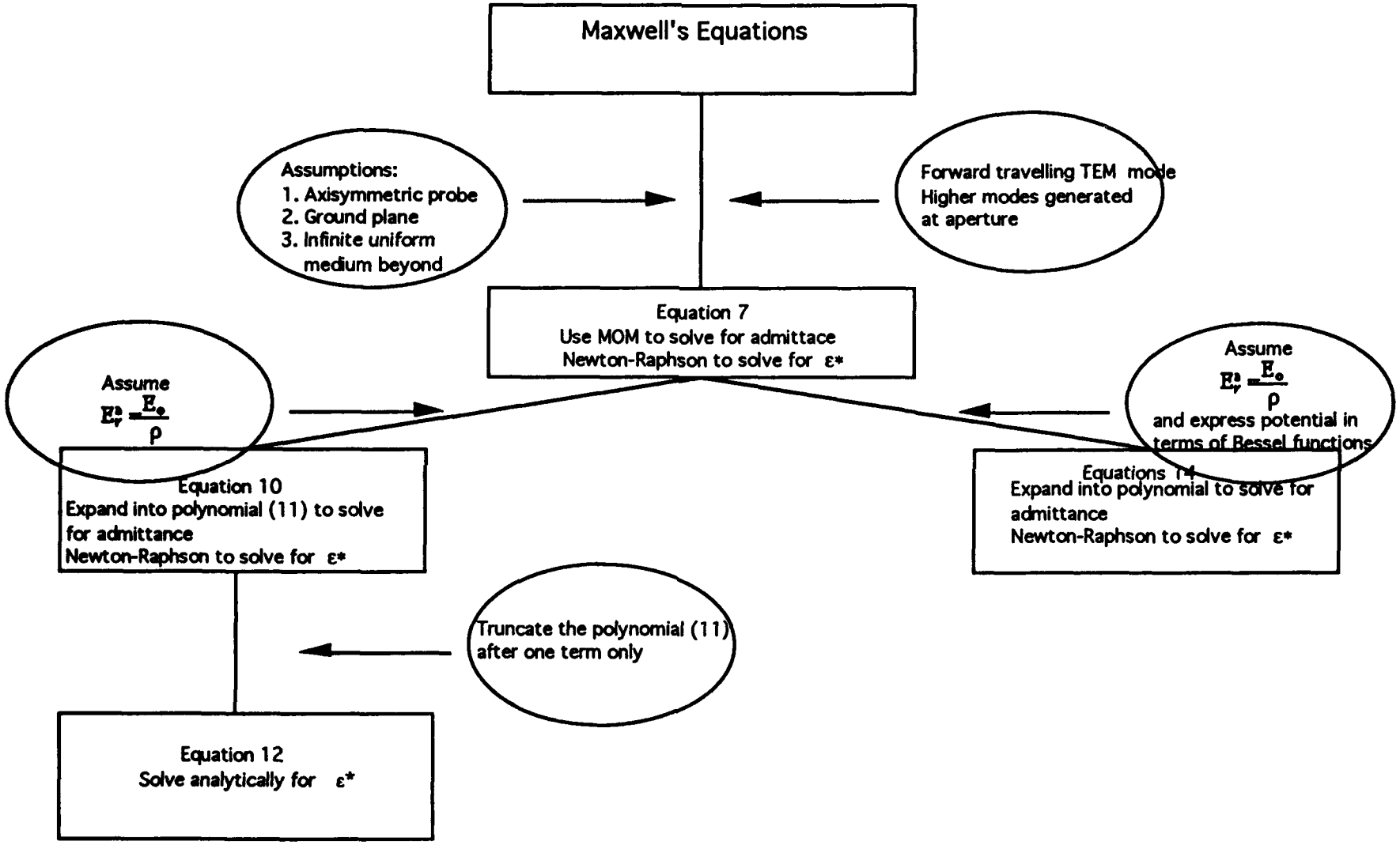

Figure 3: Derivation of admittance models for a coaxial probe

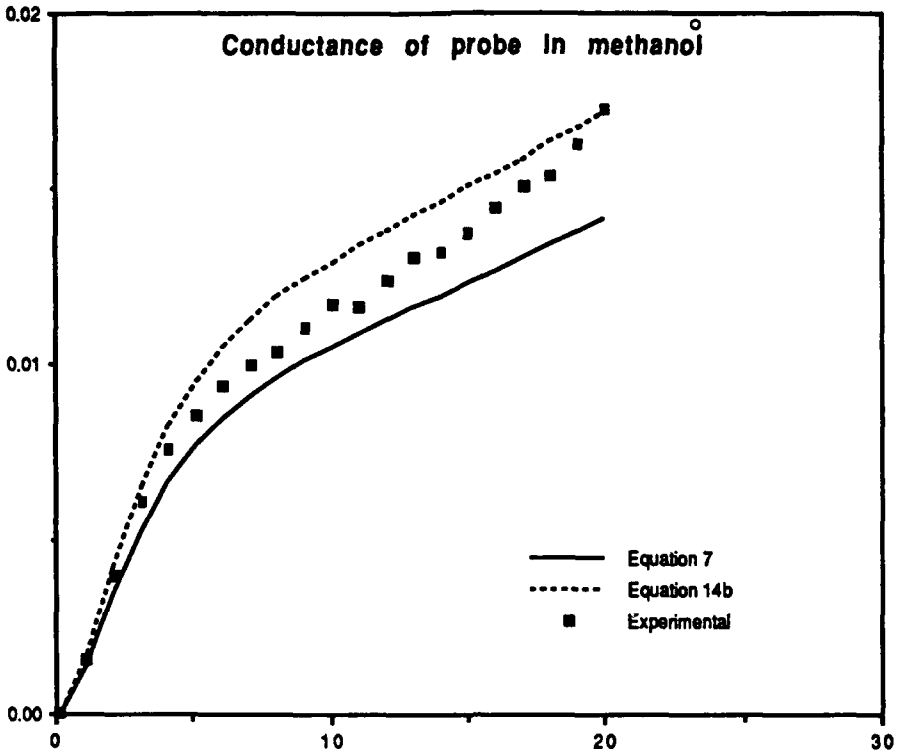

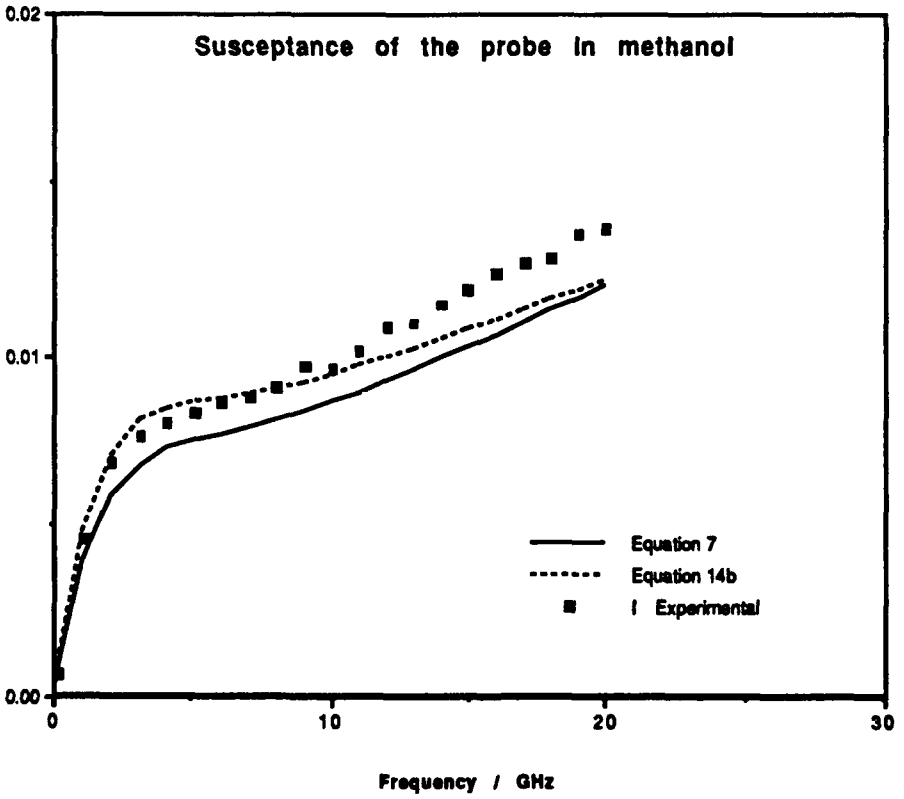

Figures 4 : (a) Real and (b) imaginary parts of the admittance of a coaxial probe in methanol at 20°C

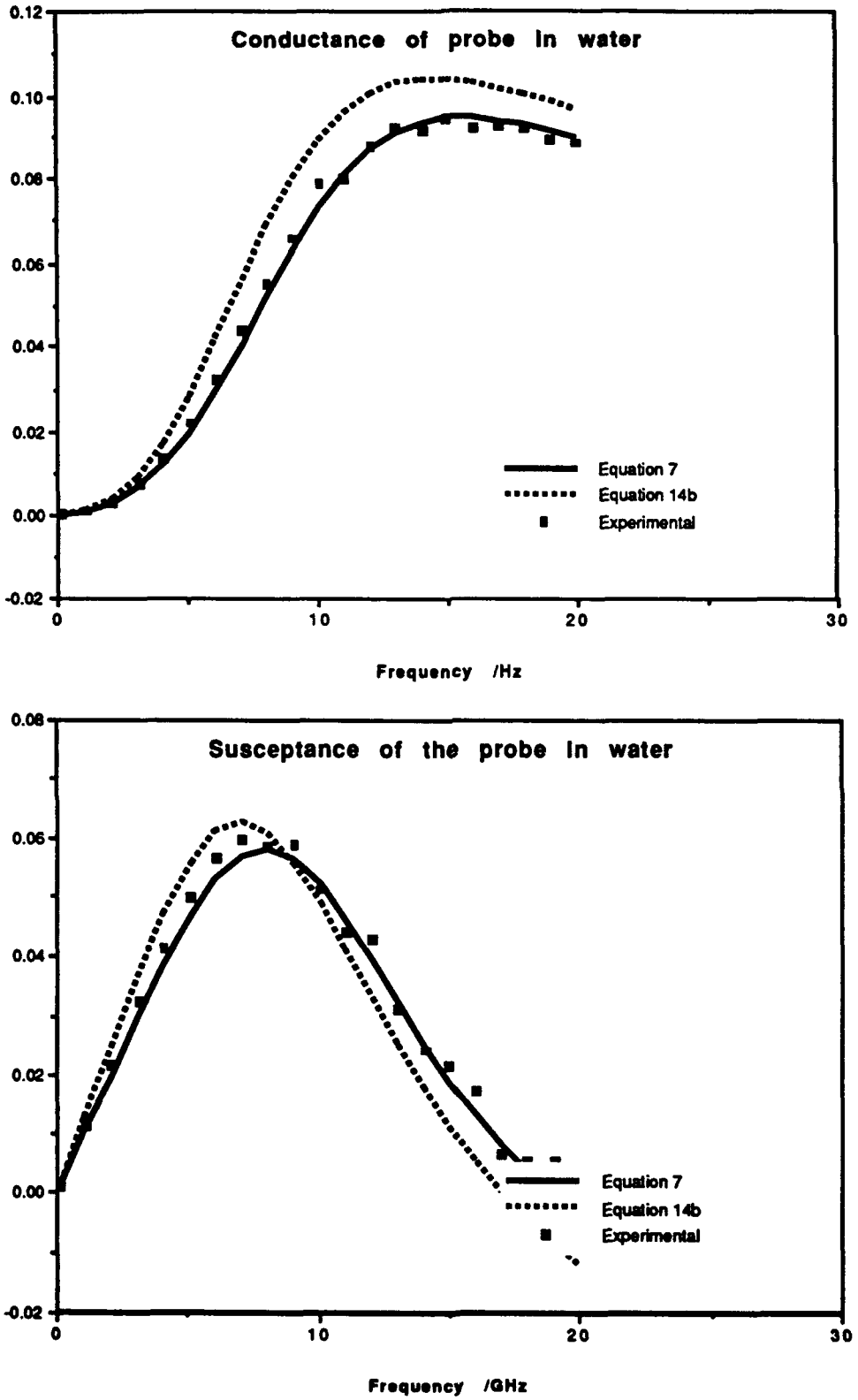

Figures 5 : (a) Real and (b) imaginary parts of the admittance of a coaxial probe in water at 20°C

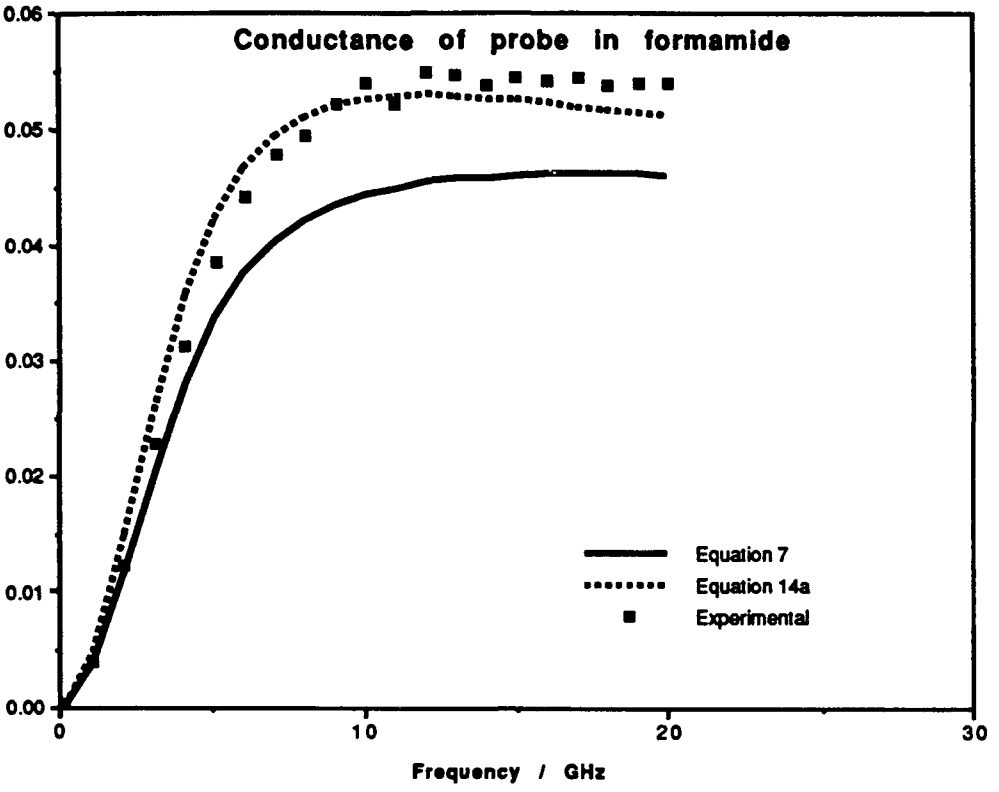

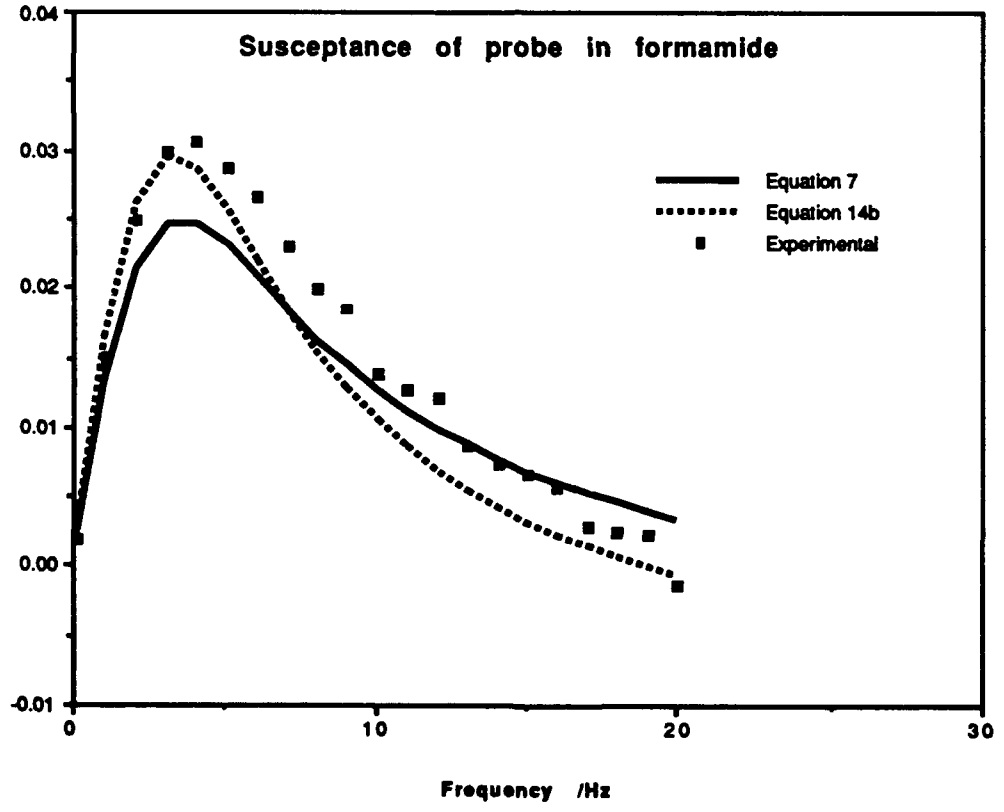

Figures 6 : (a) Real and (b) imaginary parts of the admittance of a coaxial probe in formamide at 20°C

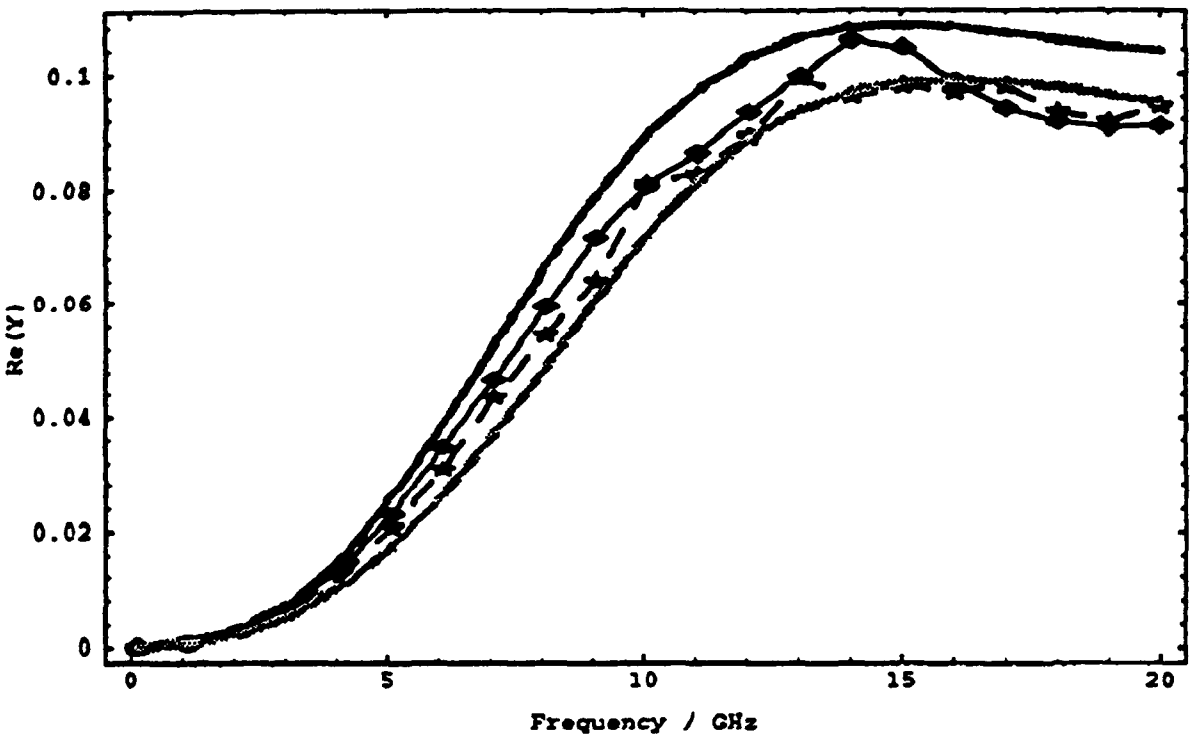

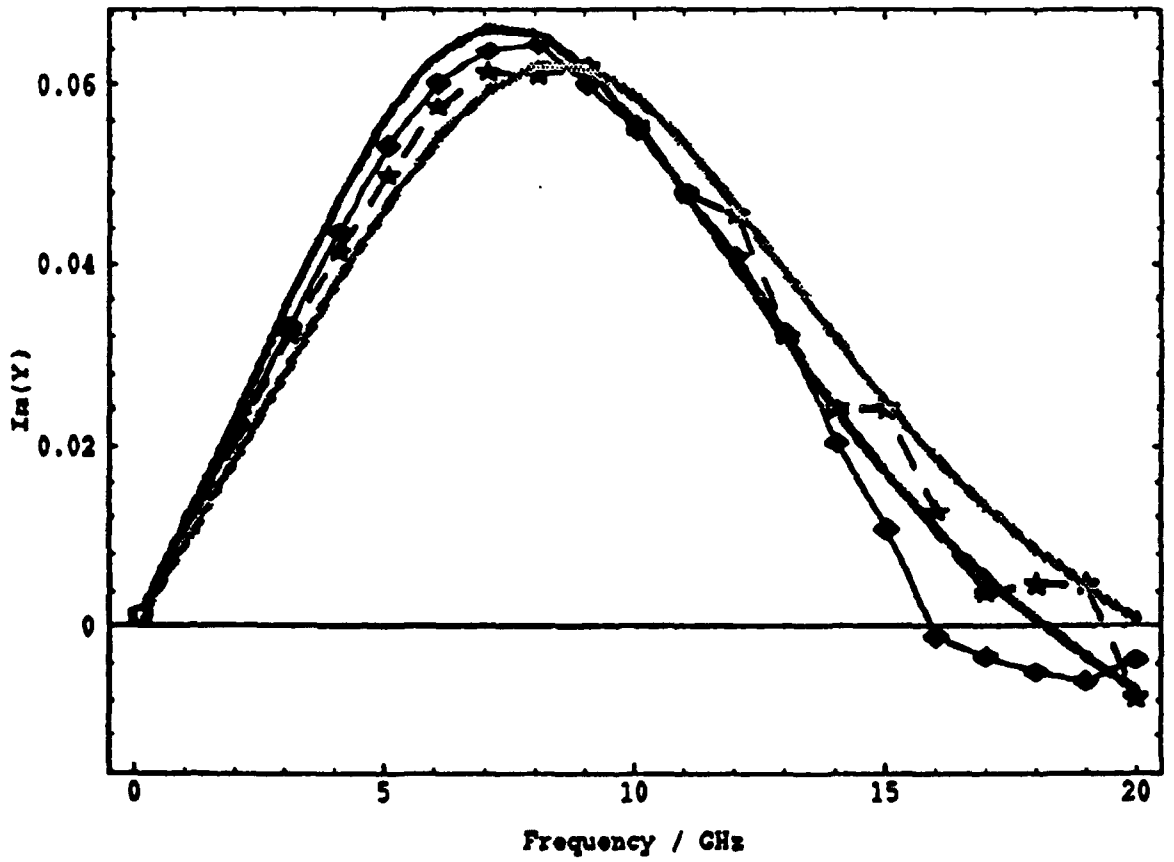

Figures 7 : (a) Real and (b) imaginary parts of the admittance of a coaxial probe in water at 23.8°C. The joined symbols are experimental measurements and the solid lines the predictions of the two models

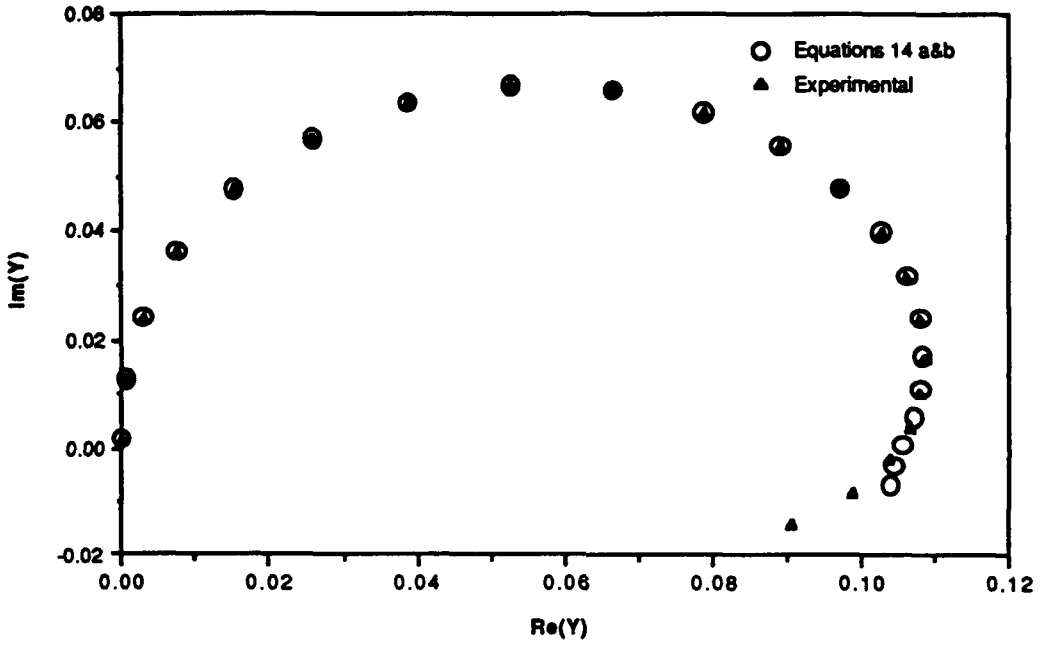

Figure 8 Measured and calculated values of the complex admittance of the probe in contact with water at 20 °C and in the frequency range 100 MHz to 20 GHz

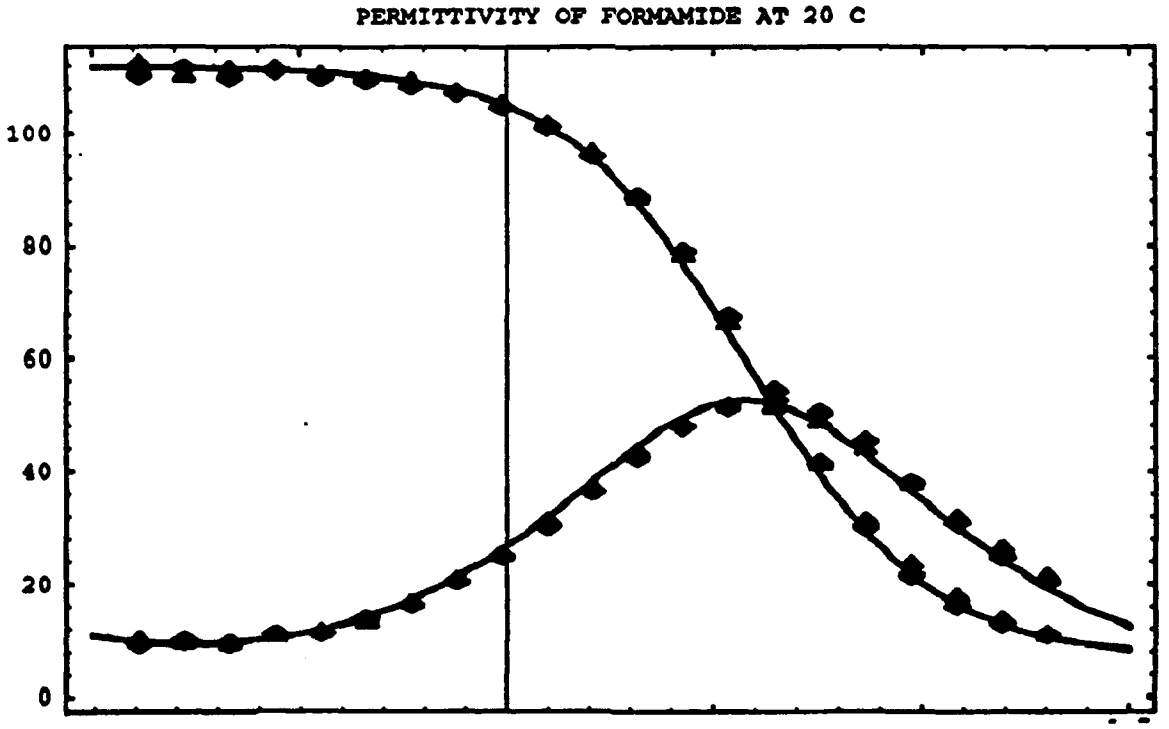

Figure 9: Measured (symbols) and literature values of the complex permittivity of formamide at 20°C